

Electron Ejection from Metals due to 1- to 10-keV Noble Gas Ion Bombardment. II. Single Crystal*

G. D. MAGNUSON AND C. E. CARLSTON

Space Science Laboratory, General Dynamics/Astronautics, San Diego, California

(Received 3 October 1962).

The secondary electron ejection coefficient has been measured for the three low-index planes of copper single crystals using a sputtering technique to maintain monatomically clean surfaces. The ion used was Ar^+ in the energy range 0.5 to 10.0 keV. The planes investigated were the (100), (110), and the (111) planes. A simple geometrical model based on the opacity of the lattice in different crystallographic directions is found to agree reasonably well with the experimental results at higher energies.

INTRODUCTION

MANY measurements have been made of γ , the ion-electron ejection coefficient, from various surfaces bombarded by many species of ions.¹ In spite of the fact that most of the measurements have been made using techniques that should result in clean surface values of γ , there is still significant disagreement between investigators. It was felt by the authors that if the surfaces used by different investigators were monatomically clean, the difference in results may have been due to differences in the targets used. Target purity does not seem to be the cause of disagreement, since one can expect that most work was done with targets of purity better than 99.9%. It does not seem likely that trace amounts of impurities will have a large effect upon γ .

There were several factors which led the authors to the investigation of γ from single crystals. One is that the photoelectric work functions are known to vary with crystal face. This, of course, would make the largest difference in the potential ejection region due to the dependence of γ on $(E_i - 2\phi)$, where E_i is the first ionization potential of the bombarding ion, and ϕ is the work function of the material. Another is that the apparent density or opacity of a crystal is different for each crystallographic direction. This might be expected to have an effect on γ at the higher energies, i.e., in the kinetic ejection range. This was thought to be so if, indeed, the kinetic ejection mechanism does involve collisions between the incoming ion (or neutral atom) and the lattice atoms with their associated bound electrons.

In addition, when a polycrystalline material is formed by rolling into thin sheets such as those used in the flashing technique, the material in general does not remain polycrystalline with random orientation of the individual crystals. There is a tendency to form preferred orientations² of the crystals of which the material is comprised. This would mean that on the average, it may be possible to have some particular orientation, say

the [100] direction, normal to the surface to a larger extent in one sample than in another. Southern *et al.*³ have seen this to be so in copper by examining a deposit spot pattern obtained from a sheet of polycrystalline copper sputtered by positive ions. Preferred orientations are well known in the field of metallurgy.⁴ Repeated heating of a metal will tend to form larger crystals in the material than were previously present.^{5,6} These crystals may become so large that the beam of ions may be incident on only one or two of the crystals. The likelihood of this happening, however, would seem to be small. One can not determine with any certainty the nature of the targets used by various investigators. It should be pointed out that when the authors used a target cut from the same sheet of 0.001-in. Mo that was used by Mahadevan, Layton, and Medved⁷ of this laboratory, remarkable agreement was observed for Ar^+ ion bombardment. The results reported in our previous paper¹ on polycrystalline secondary electron emission were for a considerably thicker target than was used by Mahadevan *et al.*,⁷ since the thin samples would erode through before a complete measurement of γ as a function of energy could be made. Although the agreement of our data¹ with those of Mahadevan *et al.*⁷ is excellent, there is an indication that their results are tending to deviate from ours at the upper end of their energy range (2.5 keV), and that their γ curve is tending to rise more steeply. We felt that this small difference could possibly be due to the thicker targets used by us and the correspondingly different crystal structure of the surface. These, then, were the factors stimulating the authors into investigation of secondary electron ejection from single crystals.

Since Cu was convenient for the authors to grow a single crystals in this laboratory, Cu was used to determine the effect of crystal orientation on the value of γ . Indeed, a variation of γ was observed that was larger than any variation seen on different materials subjected

* This research was supported in part by NASA, Lewis Research Center, Cleveland, Ohio.

¹ For a partial list of references see G. D. Magnuson and C. E. Carlston, preceding paper. [Phys. Rev. **129**, 2403 (1963)].

² C. S. Barrett, in *Metals Handbook*, edited by Taylor Lyman (American Society for Metals, Cleveland, Ohio, 1960), p. 32.

³ A. L. Southern, William R. Willis, and Mark T. Robinson, J. Appl. Phys. **34**, 153 (1963).

⁴ C. S. Barrett, *Structure of Metals* (McGraw-Hill Book Company, Inc., New York, 1952), Chap. XVIII.

⁵ See Chap. XIX of reference 4.

⁶ See the material on Mo given on p. 1140 of reference 2.

⁷ P. Mahadevan, J. K. Layton, and D. B. Medved, Phys. Rev. **129**, 79 (1963).

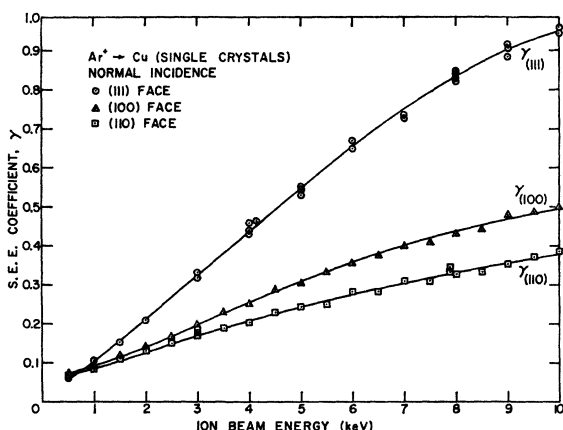


FIG. 1. Secondary electron ejection (S.E.E.) coefficient from the three low-index planes of copper due to Ar^+ ion bombardment.

to Ar^+ ion bombardment in this laboratory.¹ That is to say, our previous curves¹ for γ of Ar^+ on Cu, Ni, Al, Ta, Zr, and Mo did not show the wide variation that our results show for Ar^+ on the three low index planes of Cu.

A simple geometrical model based on the opacity of the crystal in different crystallographic directions is proposed to account for much of the observed variation in γ from different single-crystal planes.

APPARATUS AND PROCEDURE

The apparatus used in this experiment has been described in detail in the previous paper.¹ The apparatus

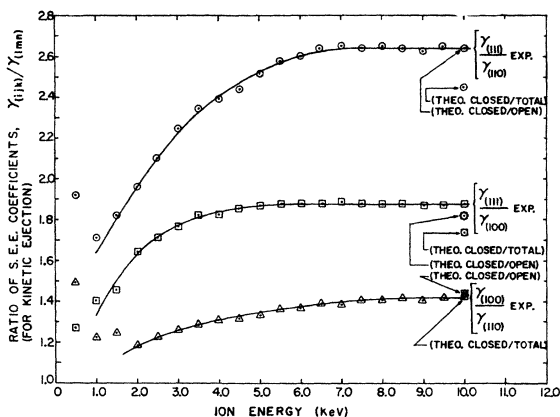


FIG. 2. The ratio of $\gamma_{(ijk)}$ to $\gamma_{(i'j'k')}$ as a function of ion energy.

consists of (1) an ion source the characteristics and operation of which have previously been reported,⁸ (2) a stainless steel target chamber 14 in. in diam and 18 in. long capable of achieving vacua of 1 to 5×10^{-8} Torr, in which background pressure the experiments were performed, and (3) a target-collector system which was

⁸ C. E. Carlston and G. D. Magnuson, Rev. Sci. Instr. 33, 905 (1962).

used to hold and orient the targets and to measure the secondary electron emission coefficient γ . See Fig. 1 of the previous paper.¹

The basic procedure for the measurement of γ has been reported in the previous paper.¹ In order to measure the secondary electron ejection coefficient for single crystals, additional procedures are necessary. These involve target growing, cutting, and orienting.

The crystals are grown from 99.999% pure copper rod stock in an induction furnace. After the orientation of the resultant boule is determined, a target slab of the proper orientation is cut from the boule by a Carborundum saw. This target slab is approximately $\frac{1}{8}$ in. to $\frac{1}{4}$ in. thick. The slab is sanded with emery paper until smooth on both sides and then etched in a weak HNO_3 solution to remove the cold-worked layers. The sample

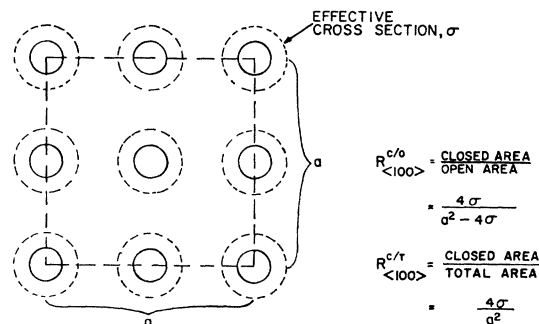


FIG. 3. Opacity of a face-centered cubic lattice as viewed from the $[100]$ direction.

is then mounted in the target holder and the target holder mounted on an XRD-5 x-ray diffraction machine. A back reflection Laue pattern is then taken. The target sample is acceptable if it is within $\pm 2^\circ$ of the proper orientation, otherwise it is discarded. The crystals used in this work were oriented within $\pm 1^\circ$, i.e., the angle between the normal to the physical surface and the desired crystallographic direction was less than 1° . The target holder is then installed in the vacuum system and aligned by means of a permanently mounted protractor to within $\frac{1}{4}^\circ$ of normal ion incidence. The basic procedure involving source preparation and vacuum conditions

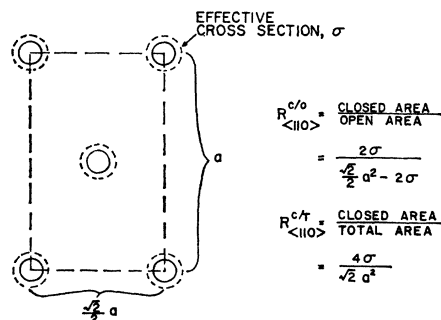


FIG. 4. Opacity of a face-centered cubic lattice as viewed from the $[110]$ direction.

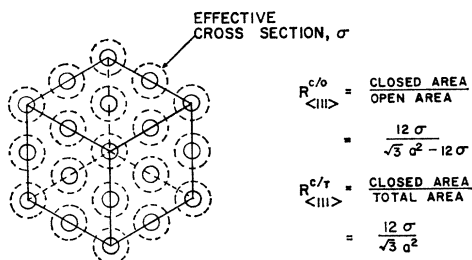


FIG. 5. Opacity of a face-centered cubic lattice as viewed from the [111] direction.

is then completed as explained in the previous paper.¹ All experimental work reported here was done in a background pressure of from 1 to 5×10^{-8} Torr and an operating pressure of 3 to 6×10^{-6} Torr.

Saturation currents to the collector and to the target were measured for both positive and negative voltages applied to the collector, with respect to target voltage. The target was grounded through an electrometer. The component of the beam which is reflected or becomes metastable atoms at the surface was assumed to produce secondary electrons and to be of high enough energy (after reflection or metastable formation) not to be retarded at the positive collector saturation voltage. γ is then given by $\gamma = (I_c + I_R) / (I_i + I_c)$. The authors feel that not enough is known about the reflection of positive ions from surfaces or about the formation of metastables at surfaces to warrant definite statements concerning their nature. The authors feel that the energy of the reflected ions involved must be either of the order of the incident beam energy or less than 100 V, because of the

SYMBOL		AREA RATIO		CRYSTALLOGRAPHIC DIRECTION		
				$\langle 111 \rangle$	$\langle 100 \rangle$	$\langle 110 \rangle$
$R_{(ijk)}^{c/o}$	CLOSED	12σ	4σ	2σ		
	OPEN	$\sqrt{3}a^2 - 12\sigma$	$a^2 - 4\sigma$	$\sqrt{2}/2 a^2 - 2\sigma$		
$R_{(ijk)}^{c/t}$	CLOSED	12σ	4σ	2σ		
	TOTAL	$\sqrt{3}a^2$	a^2	$\sqrt{2}/2 a^2$		
$R_{(ijk)}^{o/t}$	OPEN	$\sqrt{3}a^2 - 12\sigma$	$a^2 - 4\sigma$	$\sqrt{2}/2 a^2 - 2\sigma$		
	TOTAL	$\sqrt{3}a^2$	a^2	$\sqrt{2}/2 a^2$		

FIG. 6. Various area ratios for the three low-index planes of the face-centered cubic lattice. σ = collision cross section for secondary electron emission; a = lattice parameter.

flatness of the saturation electron current to the collector. The magnitude of I_R in the results reported here is small ($\sim 0.01I_i$ at 10 keV) and decreases with decreasing energy. The correction has a small effect on γ . For example, the effect at 500-eV ion energy is to increase γ by about 5%. The effect is less as energy is increased so that the 5% figure is a maximum correction factor.

Reflection coefficients have also been measured by the authors as a matter of course but will not be reported here since we have, at present, no way of determining the true nature of what we have called the reflected ion component. It is hoped that the positive saturation current to the collector will be found to be reflected ions

of high enough energy so that measurements of the true energy distributions of the secondary electrons can be made.

RESULTS AND DISCUSSION

Our measurements of γ on the three low-index planes of Cu are shown in Fig. 1. It is immediately obvious from Fig. 1 that the secondary electron emission coefficient is influenced by crystalline orientation. The tendency is that the more densely packed the metal appears to be to the incoming ion beam, the larger γ seems to be. These results, coupled with the fact that preferential orientations of rolled and drawn metals do exist lead the authors to believe that to a large extent, differences between the results of various investigators can be explained by differences in preferred orientation of the samples used as targets.

RATIO OF RATIO OF AREAS						
RATIO OF AREAS	$R_{(110)} / R_{(100)}$	LIM $\sigma \rightarrow 0$	$R_{(100)} / R_{(110)}$	LIM $\sigma \rightarrow 0$	$R_{(110)} / R_{(110)}$	LIM $\sigma \rightarrow 0$
CLOSED	$3a^2 - 12\sigma$	1.732	$\frac{\sqrt{2}a^2 - 4\sigma}{a^2 - 4\sigma}$	1.41	$\frac{3\sqrt{2}a^2 - 12\sigma}{\sqrt{3}a^2 - 12\sigma}$	2.45
OPEN	$\sqrt{3}a^2 - 12\sigma$					
CLOSED TOTAL	1.732		1.414		2.45	
OPEN TOTAL	$\frac{\sqrt{3}a^2 - 12\sigma}{\sqrt{3}a^2}$	1	$\frac{\sqrt{2}/2(a^2 - 4\sigma)}{\sqrt{2}/2a^2 - 2\sigma}$	1	$\frac{\sqrt{2}/2(\sqrt{3}a^2 - 12\sigma)}{\sqrt{3}/2(a^2 - 4\sigma)}$	1

FIG. 7. Ratios of the ratios of areas of one crystallographic direction to another. σ = collision cross section for secondary electron emission; a = lattice parameter.

The crossover of the (111) curve at lower energies cannot be explained at this time. The values of γ in the potential ejection range are not what one would expect on the basis of the known work functions of the (111) and the (100) faces of copper. Since ϕ of the Cu (111) plane⁹ is 4.86V and that of the (100) plane is 5.61 V, one would expect the potential ejection of the (111) plane to be greater than that of the (100) plane, contrary to what is observed. We can only state that evidence seems to indicate that our surfaces were clean at 500-eV ion energy. γ has been plotted vs beam flag closed time in order to obtain a monolayer formation time curve for

$X_{(ijk)} / Y_{(lmn)}$	CLOSED TO OPEN	CLOSED TO TOTAL	OPEN TO TOTAL				
EXR.	THEO.	VALUE	DEVIATION	VALUE	DEVIATION	VALUE	DEVIATION
1.89	$\frac{R_{(111)}}{R_{(100)}}$	1.84	2.8%	1.73	8.5%	1.88	0.5%
2.68	$\frac{R_{(100)}}{R_{(110)}}$	2.67	0.5%	2.45	8.6%	2.73	1.9%
1.41	$\frac{R_{(111)}}{R_{(110)}}$	1.45	2.8%	1.41	0	1.49	5.7%
	COLLISION CROSS SECTION FOR RESISTANCE	25×10^{16} cm ²		ANY		28×10^{16} cm ²	
	COLLISION RADIUS	0.284 Å		ANY		3.02 Å	

BOHR RADIUS AT 10keV = 0.225 Å

FIG. 8. Comparison of experimental results with the results expected on the basis of a simple geometrical model at 10-keV ion energy.

⁹ N. Underwood, Phys. Rev. 47, 502 (1935).

all three of the faces for which γ is reported here. In addition, γ vs beam current density curves have been obtained for two of the three low index planes, namely the (110) face, which has the lowest sputtering rate of the three planes, and the (111) face, which has the highest sputtering yield. Figure 2 of the previous paper¹ shows the dependence of γ on beam current density for the (110) face and Fig. 3 of the previous paper¹ shows the monolayer formation time curve for the (110) face.

When the ratios $\gamma_{(111)}/\gamma_{(110)}$, $\gamma_{(111)}/\gamma_{(100)}$, and $\gamma_{(100)}/\gamma_{(110)}$ are plotted as in Fig. 2 one sees that the ratios approach a constant value. This seemed to indicate that there might be a simple geometrical property of the crystal faces that causes the differences in $\gamma_{(ijk)}$. We, therefore, examined the appearance of the crystal faces as they would appear to an incoming ion. Examining the (100) face of the face-centered cubic lattice (Fig. 3) and assuming that some collision cross section (denoted by σ) is associated with each atom we see that each corner atom contributes $\frac{1}{4}\sigma$ to the total closed area of the face. Each face-center atom located a distance $a/2$ below the surface contributes $\frac{1}{2}\sigma$. Finally, the face-center atom located on the surface contributes σ . The total closed area is given by $4 \times \frac{1}{4}\sigma + 4 \times \frac{1}{2}\sigma + \sigma = 4\sigma$. The ratio of closed area to total area is then $R^{e/T} = 4\sigma/a^2$, where a is the lattice parameter. The closed-to-total-area ratio represents the fraction of the beam which has a collision in the first layers of the crystal that can result in secondary emission of an electron. The closed-to-open area ratio would be $R^{e/o} = 4\sigma/(a^2 - 4\sigma)$. Figures 4 and 5 show the face-centered cubic lattice as it appears to an incoming ion for the [110] direction and the [111] direction, respectively. Results of the calculations of the ratios of closed to total and closed to open areas for the three low-index directions are given in Fig. 6.

We have formulated a simple geometrical model to try to explain our results. The assumptions we make are the following:

- (1) Secondary electron emission involves an inelastic collision between an incoming ion and a lattice atom.
- (2) An incoming ion either makes a collision with one of the atoms near the surface (i.e., before the lattice repeats) or it passes deeply enough into the lattice to be ineffective in producing secondary electrons.
- (3) The probability of escape for an electron from the surface is the same for all three faces. This is not strictly true, but since we are assuming that the collision occurs so close to the surface this assumption cannot be too much in error.
- (4) γ is linearly proportional to the probability of collision for each incoming ion. That is, if only $\frac{1}{10}$ of the area facing an incoming ion is closed, then only $\frac{1}{10}$ of the beam will be effective in producing secondary electrons.

If γ is proportional to $R^{e/T}$, then we can take the ratio of $\gamma_{(ijk)}$ to $\gamma_{(i'j'k')}$ and it should be the same as the ratio of the closed to total area ratios for the two directions, for example, $\gamma_{(111)}/\gamma_{(110)} = R_{(111)}^{e/T}/R_{(110)}^{e/T}$.

Figure 7 shows the values for the ratios of the ratios of the areas. For small cross sections at high energies $R^{e/o}$ approaches the value of $R^{e/T}$. The ratios $R_{(i,j,k)}^{e/T}/R_{(i',j',k')}^{e/T}$ are constant for energies above which the cross section is small enough so that no overlapping of the closed areas is in evidence. It seems likely that in Fig. 2, the plot of the ratios of γ vs energy, the drop-off of the curve at lower energies is evidence of the overlapping of the closed areas.

Figure 8 shows a comparison of our experimental results at 10 keV with the results predicted by the simple geometrical model we have proposed. The results for the closed to total values agree within the experimental uncertainty in the data. However, at 10 keV σ is small enough so that the closed-to-open ratio is very nearly the same as the closed-to-total ratio. One can, therefore, calculate a cross section at 10 keV and it agrees quite well with the value predicted using a Bohr collision radius¹⁰ for Ar⁺ on Cu. Our calculated result is some 26% larger than the Bohr collision cross section. The value of σ calculated was of such value to obtain the best agreement with the experimental results.

The values of the open area to total area were also calculated to test whether the collisions resulting in secondary emission could be between the incoming ion and the free electron gas of the metal. As expected, the results discount this possibility. Calculating a collision cross section from the open-to-total-area ratio results in an extremely large cross section, and for this reason it does not seem likely that the open-to-total ratio enters into the determination of γ , even though this large cross section will give good agreement with the experimental results.

We conclude from the above that although the opacity model is a very simple geometrical model, there may be some validity for its use in interpreting the mechanism of secondary emission in the kinetic ejection range. We conclude that most likely the mechanism does involve the collisions of ions with lattice atoms resulting in the excitation and eventual ejection of bound electrons.

We further conclude that the difference in γ for each of the three surfaces may, in large part, be explained by the differences in opacity of the three low-index faces.

Finally, we conclude that on the basis of our data and references 2 to 6 on crystal growth and preferred orientation that past history of the target sample can explain to a large extent the differences in the γ of polycrystalline materials as found by various investigators.

¹⁰ N. Bohr, Kgl. Danske Videnskab. Selskab, Mat.-Fys. Medd. 18, No. 8 (1948).